Planta (2020) 251:44
https://doi.org/10.1007/s00425-019-03326-9

ORIGINAL ARTICLE

MicroRNA-mediated responses to colchicine treatment in barley

Fang-Yao Sun[1] · Lin Liu[1] · Yi Yu[1] · Xin-Ming Ruan[1] · Cheng-Yu Wang[1] · Qun-Wen Hu[1] · De-Xiang Wu[1] · Genlou Sun[2]

Received: 25 August 2019 / Accepted: 6 December 2019 / Published online: 6 January 2020

Abstract

Main conclusion **In *Hordeum vulgare*, nine differentially expressed novel miRNAs were induced by colchicine. Five novel miRNA in colchicine solution showed the opposite expression patterns as those in water.**

Abstract Colchicine is a commonly used agent for plant chromosome set doubling. MicroRNA-mediated responses to colchicine treatment in plants have not been characterized. Here, we characterized new microRNAs induced by colchicine treatment in *Hordeum vulgare* using high-throughput sequencing. Our results showed that 39 differentially expressed miRNAs were affected by water treatment, including 34 novel miRNAs and 5 known miRNAs; 42 miRNAs, including 37 novel miRNAs and 5 known miRNAs, were synergistically affected by colchicine and water, and 9 differentially expressed novel miRNAs were induced by colchicine. The novel_mir69, novel_mir57, novel_mir75, novel_mir38, and novel_mir56 in colchicine treatment showed the opposite expression patterns as those in water. By analyzing these 9 differentially expressed novel miRNAs and their targets, we found that novel_mir69, novel_mir56 and novel_mir25 co-target the genes involving the DNA repair pathway. Based on our results, microRNA-target regulation network under colchicine treatment was proposed, which involves actin, cell cycle regulation, cell wall synthesis, and the regulation of oxidative stress. Overall, the results demonstrated the critical role of microRNAs mediated responses to colchicine treatment in plants.

Keywords Abiotic stress · Chromosome doubling · Colchicine · DNA repair pathway · *Hordeum vulgare*

Abbreviations

HV0	Barley, untreated
HV5CK	Barley, 5 h water treatment
HV5TR	Barley, 5 h colchicine treatment
NFYA5	Nuclear factor YA family
TPM	Transcripts per million

Introduction

Polyploidization is a common phenomenon in the evolution of plants. Compared with diploid plants, polyploid plants are more tolerant and adaptable to the environment, such as resistance to abiotic stress and stronger vitality (Liu and Sun 2017; Wei et al. 2018; Zhou et al. 2019). Based on these characteristics, to cope with the needs of modern agricultural production, a variety of chemicals has been used for artificial chromosome set doubling, including colchicine, trifluralin, oryzalin, amiprophos-methyl and carbamate, etc. As the best agent to induce polyploids, colchicine acts on most plants and many parts of them, such as seeds, stem growth points, scion and callus (Li et al. 2007; Zhang et al. 2007). Colchicine has widely been used in the study of cytology, genetics and plant breeding (Heinz and Mee 1970; Pan et al. 1993; Dhooghe et al. 2011), after the first success of doubling the chromosome number of plants such as in *Datura* in 1930s (Blakeslee and Avery 1937).

Colchicine, as a mitotic inhibitor, causes the chromosome to stagnate in anaphase and cytokinesis of division mainly by inhibiting the formation of the spindle. Then the cells do

Electronic supplementary material The online version of this article (https://doi.org/10.1007/s00425-019-03326-9) contains supplementary material, which is available to authorized users.

✉ Cheng-Yu Wang
wangchengyu@ahau.edu.cn

✉ De-Xiang Wu
dexiangwu198@ahau.edu.cn

✉ Genlou Sun
genlou.sun@smu.ca

[1] College of Agronomy, Anhui Agricultural University, Hefei 230036, Anhui, China

[2] Biology Department, Saint Mary's University, Halifax, NS B3H 3C3, Canada

not split during the chromatid segregation (mitotic anaphase or anaphase II) or chromosome segregation (anaphase I), thus doubling the chromosome set. With the extensive use of colchicine and the discussion of mechanism (Dhooghe et al. 2011), it has been demonstrated that colchicine binds with α- and β- tubulin dimers (Nogales et al. 1998), resulting in the depolymerization of microtubules. During mitosis, the microtubules can form a spindle, the microtubule silk extends from the spindle onto the chromosomal kinetochore, and then pulls the chromosomes toward the poles of cell. The binding of colchicine to tubulin dimer will inhibit the microtubule polymerization, thereby affecting the formation of microtubules (Hastie 1991; Nogales et al. 1998), leading to the inability of the spindle to form and the cells to divide.

Environmental stresses can induce misfolded protein aggregation in plant cells, while colchicine treatment suppressed misfolded protein aggregation in cultured grape and tobacco cells that were exposed to environmental stresses (Nakajima and Suzuki 2013). A recent transcriptome analysis showed, when plants were treated with colchicine, colchicine inhibits the expression of genes related to microtubules as well as to cytokinesis, and significantly restrains the process of membrane, cellulose, chromatid separation and cell wall development, which delayed cell activity, caused the occurrence of advanced apoptosis and could reduce the damage of waterlogging (Zhou et al. 2017). Although the scientific community today considered that colchicine generally prevents cell division by inhibiting the formation of microtubules, the molecular mechanism on how plants respond the colchicine treatment is still unclear.

MicroRNAs (miRNAs) are a class of non-coding small RNA molecules which bind to mRNA in a complementary base-pairing manner, and participate in regulating gene expression via degradation of its target gene(s) or translational inhibition (Winter and Diederichs 2011; Iwakawa and Tomari 2013). Many studies have shown that the expression of miRNA has a close relationship with the growth and development of plants, and the loss of its function will affect the growth and development of plants, such as plant size, flowering time and plant fertility (Liu et al. 2009). Several miRNAs were found to mediate the formation of plant stem cells. As examples, miR165/miR166 target class III homeodomain leucine zipper transcription factors (HD-ZIP III) to regulate the development of stem apex meristem (SAM) of mutant plant (Liu et al. 2009). miR394, synthesized in the epidermis, maintained the SAM formation of stem cells by acting as a mobile signaling molecule (Knauer et al. 2013). Other miRNAs, such as miR393 overexpressed in rice prolongated main root and increased the number of lateral roots (Bian et al. 2012). In addition, miR847 participates in plant root development by regulating gene *IAA28* expression (Wang and Guo 2015). Recent studies have also shown that miRNAs play an important role in a variety of biotic and abiotic stresses (Zhang and Wang 2015). For example, miR156 can enhance the heat resistance of *Arabidopsis* (Stief et al. 2014), miR169 can improve drought resistance and nitrogen utilization rate of tomato (Zhang et al. 2011; Zhao et al. 2011), miR319 can significantly improve the ability of plants to resist various adversities (Sunkar and Zhu 2004; Yang et al. 2013).

Colchicine is a toxic alkaloid and secondary metabolite, and becomes toxic as an extension of its cellular mechanism of action via binding to tubulin (Finkelstein et al. 2010). The affected cells will undergo impaired protein assembly with reduced endocytosis, exocytosis, cellular motility (Finkelstein et al. 2010). The common practice for using colchicine to double the chromosome set of plants is to soak plant tissue in colchicine solution (Barnabás et al. 1999; Petersen et al. 2002), in which treated plants will respond to water, colchicine, and combination of water and colchicine stress. It was reported that miRNAs have played critical role in regulating cell response to various biotic and abiotic stress, and a key role in plant growth and development. Various plant growth and development and stress related miRNAs have been identified in different plants (Liu et al. 2009; Zhao et al. 2011; Chen et al. 2012; Knauer et al. 2013). However, microRNA-mediated responses to colchicine treatment in plants has not been characterized. To address this important scientific question, and reveal the regulating role of miRNA during colchicine treatment, high throughput microRNA analysis was performed to identify novel miRNAs that responded to colchicine treatment in diploid barley (*Hordeum vulgare* L.). MicroRNA-target regulation network under colchicine treatment was proposed. The results will enhance our understanding the critical role of microRNAs mediated responses to colchicine treatment in plants.

Materials and methods

Colchicine treatment

The diploid plant seed of *Hordeum vulgare* L '11z37' ($2n = 2x = 14$) was provided by the Agricultural College of Anhui Agricultural University (China), and was germinated in a constant temperature and humidity chamber and a humidity of 75%. The germinated seeds were transferred to a foam grid board with uniform plant density for hydroponic culture. The foam grid broad was placed on a plastic box. The seedlings were suspended on a modified Hoagland solution. The roots were immersed in a constantly aerated nutrient solution, and transferred it to an artificial climate chamber for growth at a temperature of 22/16 °C (day/night), relative humidity of 65–75%, and the photoperiod was 14 h/10 h dark/light. After the plant grew to the 3–4 leaf stage, the whole plant was taken out of the plastic box and

the residual nutrient solution was gently washed away using running water. The '11z37'seedlings were randomly divided into two groups with three replicates for each group. One of these groups was grown in water and another group was treated with the mix of 2.5 mM colchicine (0.1%, w/v) and 2% dimethyl sulfoxide (DMSO) (Sourour et al. 2014). Roots of samples in each group were separated randomly into more than 3 sub-groups, each with a few dozen of plants. Roots tissues were harvested from each sub-group at the time of 0 h and 5 h, and preserved immediately in liquid nitrogen for RNA isolation.

RNA extraction and high-throughput sequencing

Total RNA was extracted from approximately 100 mg of root using TRIzol reagent according to the manufacture's protocol (Sangon Biotech, Shanghai, China). Nine RNAs samples (HV0: 0 h, non-treated; HV5hCK: 5 h, water treated; and HV5hTR: 5 h, colchicine treated, each with three replicates) of the variety '11z37' were sent to the BGI (BGI Shenzhen Corporation, Shenzhen, China) for sequencing using the BGI-seq 500 platform.

Bioinformatics identification of novel and conserved miRNAs

As described by Sunkar et al. (2005), we removed impurities from the original data, including no insert fragment sequences, sequences with too long insert fragment, low quality sequences, poly A sequences and small fragment sequences. Clean reads were mapped onto the reference genome and other miRNA databases using Anchor Alignment Based Small RNA Annotation (AASRA) software. The aligned small RNA was uploaded to the miBase 22.0 database to identify known miRNAs. Based on the miRNA-precursor can form a hairpin secondary structure, we used the miRA software to identify the novel miRNA using the minimum folding free energy index (Evers et al. 2015). In addition, to compare the common and unique miRNAs in different libraries, the Venn program was used to generate Venn diagrams. The expression criteria of each miRNA were converted into transcripts per million (TPM) according to the following formula: TPM = actual miRNA count/clean readers × 1,000,000 based on the standardized expression of each miRNA in the three libraries; RStudio Team (2015) was used to generate heat maps to compare the expression of miRNA among the three libraries.

miRNA differential expression analysis

To compare the miRNA abundance among the three sets of libraries and identify the differentially expressed miRNAs based on the number of genomic tags in each sample, we used TPM to normalize the expression level of small RNAs, since this kind of treatment can avoid the effect of quantitative accuracy of different sequencing amounts: TPM = $(C \times 10^6)/N$, of which C represents the copy number of a certain miRNA in the sample, and N represents the total number of genomes on that certain sample. The normalized data were used for the subsequent differentially expression comparison analysis. The fold change was calculated using fold change = log2 (miRNA TPM in HV5hTR/miRNA TPM in HV5hCK). Positive values indicated upregulation of miRNA, while negative values indicated downregulation of miRNA. To identify genes specifically expressed, the P value of each gene was corrected by multiple hypothesis tests using Q value. Genes that conform to the double or more differences and the Q value that is less than or equal to 0.001 were considered to be significantly differentially expressed genes. Volcano maps were generated using RStudio Team (2015) to identify differentially expressed miRNAs among treatments and control.

Verification of miRNA and target genes using qRT-PCR

The miRNA tailing reverse transcription primer was designed according to the method of Shi and Chiang (2005), and used for the transcription of total RNA. The cDNA was then used for qRT-PCR using specific forward primers and universal reverse primers (10 µM). Reverse transcription was performed using miRNA First Strand cDNA Synthesis-Tailing Reaction (Sangon Biotech, Shanghai, China) according to the manufacturer's recommendation. The 18S rRNA was used as an internal reference for tailing qRT-PCR. Quantitative real-time PCR was performed using a Bio-Rad CFX-96 Touch (Bio-Rad, Hercules, CA, USA). Each 20 µl reaction contained 10 µl 2 × miRNA qPCR master mix; 0.5 µl (10 µM) forward primer; 0.5 µl (10 µM) reverse primer; 7 µl RNase-free water and 2 µl cDNA template. The PCR procedure was 95 °C for 30 s, followed by 40 cycles of 95 °C for 5 s and 60 °C for 30 s. After the reaction was completed, a melting curve was set to evaluate primer specificity. All reactions were performed in triplicates. Relative expression levels were calculated using the $2^{-\Delta\Delta CT}$ method (Pfaffl 2001).

Thirty-three target genes were selected to verify their expression in '11z37' 5 h samples. The primers of the target gene were designed using Primer 3.0.4.0 (Untergasser et al. 2012). Suitable primers were selected for final PCR experiments based on their specificity and amplification efficiency. TransScript II Green one-step qRT-PCR SuperMix (Transgen Biotech, Beijing, China) was used to prepare cDNA by reverse transcription. A total of 20 µl of each reaction contained 10 µl 2 × TransStart Tip Green qPCR SuperMix (Transgen Biotech), 2 µl cDNA template, 0.4 µl

forward primer, 0.4 µl reverse primer, and 7.2 µl RNase-free water. The qRT-PCR was run in 96-well plates using Bio-Rad CFX-96 Touch (Bio-Rad) real-time fluorescence quantification system. qPCR amplification procedure was 94 °C for 30 s, followed by 40 cycles of 94 °C for 5 s and 55 °C for 15 s, 72 °C for 10 s. The melting curve was set to assess primer specificity. Three technical replicates were set for each qPCR reaction. The average relative expression ratio was calculated using the $2^{-\Delta\Delta CT}$ method, and 18S rRNA was used as a reference gene.

Target gene prediction and GO function analysis

psRNAtarget and TargetFinder were used to predict potential targets of all miRNAs. For the TargetFinder program, prediction score cutoff value 4 was used for target prediction. For the psRNATarget program, the following parameters were used: position after which with gap/bulge permit 17, number of processors to 8, and number of gaps/bulges permitted (Katiyar et al. 2015). The jvenn program was used to draw Venn diagram (Bardou et al. 2014). After finding the target of miRNAs, the GO::TermFinder (http://www.yeastgenome.org/help/ analyze/go-term-finder) was used for enrichment analysis. The target genes were divided into three parts using the GO function package of RStudio Team: biological processes, molecular functions, and cellular components.

Results

Data analysis of sequences

To identify and predict the miRNAs associated with colchicine treatment in plants, three small RNA libraries were constructed using the RNA isolated from cultivated barley that was grown under normal growth (HV0), 5 h water treatment (HV5CK), and 5 h 0.1% colchicine solution treatment (HV5TR), and sequenced. After filtering and removing the sequences of low quality tags, adaptors, shortages, and adaptor–adaptor ligation, we obtained 118644191, 101969804, 116439374 pure reads from HV0, HV5CK, HV5TR, respectively. In Rfam database, the BLASTN program was used to search for the clean tags of these three libraries. The number and proportion of different types of small RNAs from these three libraries were given in Tables S1–S3.

The sequence lengths of different small RNAs are important features to distinguish them. Generally, the lengths of small RNAs range from 18 to 30 nt, and the peak of length distribution can help us judge the type of small RNA. The results showed that most of the small RNAs in these three libraries were 18 nt and 19 nt, followed by 20 nt and 16 nt (Fig. S1). The small RNA of 16nt length is the most abundant in the HV5TR library (Fig. S1c).

Identification of conserved miRNA and novel miRNA

Forty-six conserved miRNAs and 75 novel miRNAs were identified and predicted from the HV0 library. In HV5CK library, 38 known conserved miRNAs and 74 novel miRNAs were identified and predicted, 40 known conserved miRNAs and 75 novel miRNAs were identified and predicted in HV5TR library (Fig. 1a). A total of 54 known conserved miRNAs and 76 novel miRNAs were found from these three libraries, of which 34 known conserved miRNAs and 73 novel miRNAs were shared among the three libraries. There are 36 known conserved miRNAs and 74 novel miRNAs shared by HV0 and HV5CK. The HV0 library and the HV5TR library have the same 39 known miRNAs and 74 novel miRNAs, while the HV5CK and HV5TR shared 34 known conserved miRNAs and 73 novel miRNAs. Of the three libraries, 54 known conserved miRNAs belong to 12 miRNA families. There was no large-scale change in miRNA expression patterns between water treatment and colchicine treatment (Fig. 1b).

Differentially expressed miRNAs in the comparison of HV5CK vs HV0 and HV5TR vs HV0

To identify miRNAs induced by water, as well as combination of water and colchicine stress, the expression of each miRNA in HV5CK vs HV0 and HV5TR vs HV0 was compared. Multiple changes of each miRNA were calculated according to the following formula: fold change = log2 (miRNA TPM in the library of HV5CK or HV5TR/miRNA TPM in library HV0). The results showed that there were 39 and 42 differentially expressed miRNAs in HV5CK vs HV0 and HV5TR vs HV0, respectively (Fig. 2a, b). Compared with untreated HV0, 18 and 24 novel miRNAs were up-regulated in HV5CK and HV5TR, respectively. Two known miRNAs were up-regulated in both HV5CK and HV5TR, while 16 and 13 novel miRNAs were down-regulated in HV5CK and HV5TR, respectively. Three known miRNAs were down-regulated in both HV5CK and HV5TR. Total of 29 novel miRNAs and 5 known miRNAs were shared by HV5CK vs HV0 and HV5TR vs HV0 (Fig. 2c). Among the two comparisons, 11 novel miRNAs and 3 known miRNAs were down-regulated, and 17 novel miRNAs and two known miRNAs were up-regulated, while one novel miRNA showed opposite expression pattern.

Differentially expressed miRNA between HV5TR and HV5CK

To identify miRNAs induced by colchicine, the following formula was used to calculate the multiple changes of each miRNA between plants treated with 0.1% colchicine solution for 5 h and plants treated with water for 5 h: the

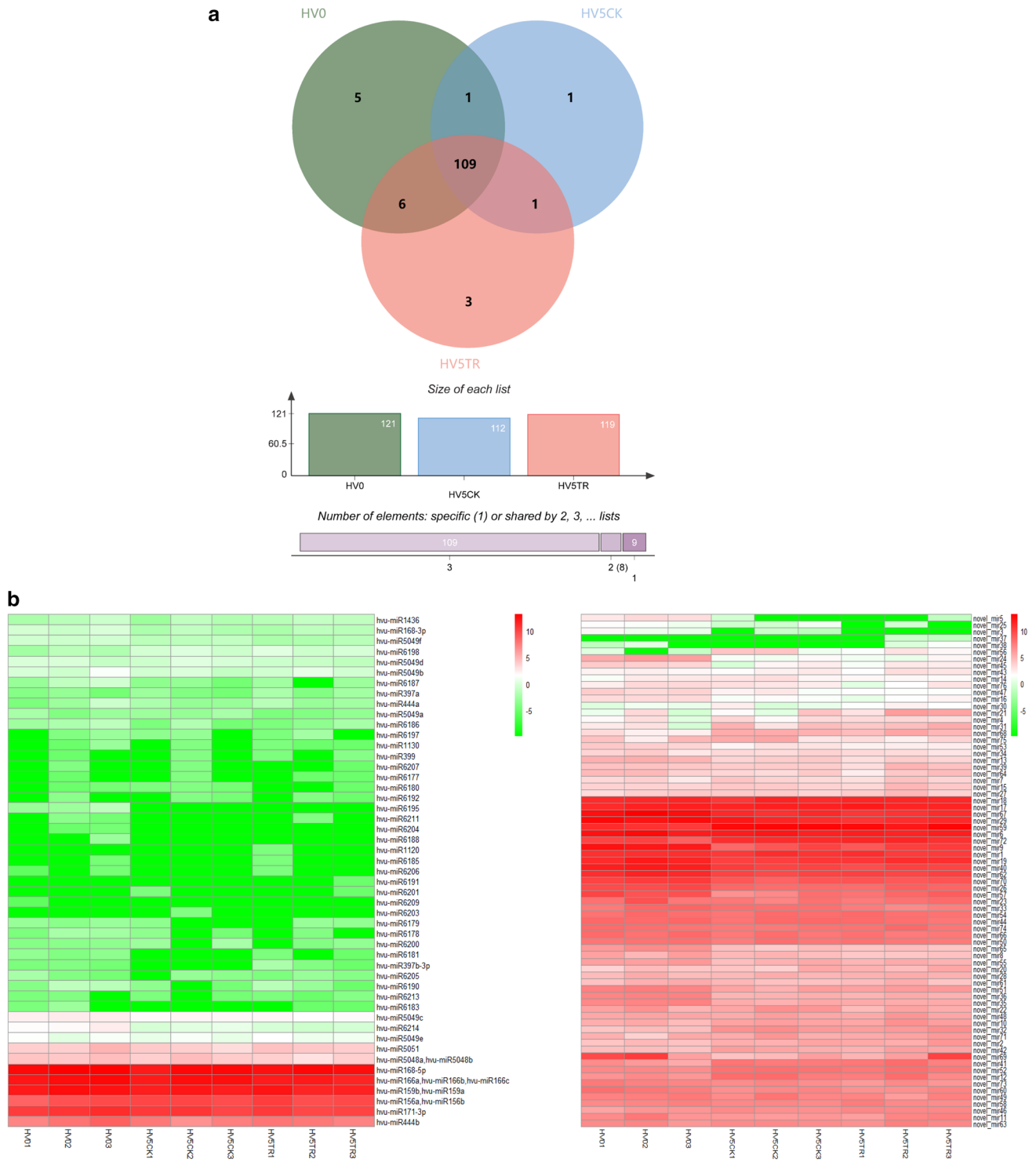

Fig. 1 The identification and expression of miRN in different libraries. **a** Venn diagram showing the number of common and unique miRNAs in normal growth (HV0), 5 h treatment in water (HV5CK), and 5 h treatment in colchicine solution (HV5TR). The following bar graph showed all of the miRNAs in each library (HV0, HV5CK, HV5T R). **b** Heat map of the expression levels of each miRNA in three different libraries (including 3 biological replicates): HV0, HV5CK, HV5TR. Different colors indicate different expression levels, as shown in the scale

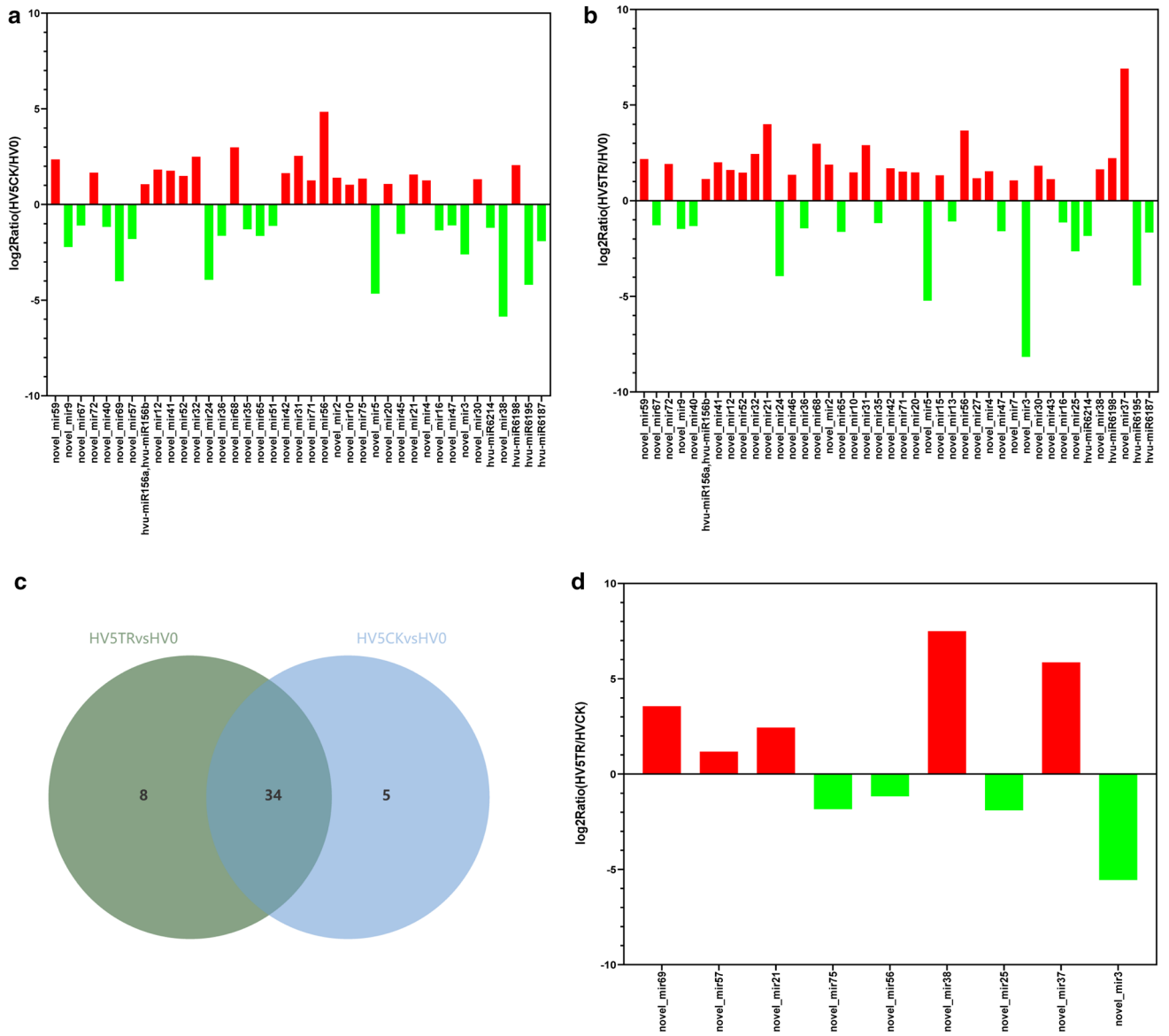

Fig. 2 The identification of differentially expressed miRNAs between water treatment and colchicine treatment. Red colour represents up-regulation and green represents down-regulation. **a** The histogram showed differentially expressed miRNAs caused by water treatment by comparing microRNA expression patterns between HV5CK and HV0. **b** The histogram showed the expression pattern of miRNAs under treatment with colchicine solution. **c** The Venn diagrams of differentially expressed miRNAs between different comparisons. **d** The histogram showed the differential expression of microRNAs caused by colchicine via analyzing the expression pattern of miRNA between colchicine treatment and water treatment

multiple changes = log2 (miRNA TPM in HV5TR/miRNA in HV5CK). Nine differentially expressed miRNAs were identified in HV5TR vs HV5CK (Table S4). Compared with HV5CK, five up-regulated novel miRNAs and four down-regulated novel miRNAs were identified in HV5TR (Fig. 2d). By analyzing the differentially expressed miRNAs and comparing these miRNAs with those in 5 h water treatment, we found that four novel miRNAs (novel_mir21, novel_mir56, novel_mir38, novel_mir3) were differentially expressed between HV5CK vs HV0 and HV5TR vs HV0; which were more influenced by colchicine (Table S4). Three novel miRNAs (novel_mir69, novel_mir57, novel_mir75) were only differentially expressed in HV5CK vs HV0; one novel miRNA (novel_mir25) was only differentially expressed in HV5TR vs HV0, and only one novel miRNA (novel_mir37) was detected and differentially expressed in HV5TR vs HV0.

Two novel miRNAs (novel_mir25, novel_mir37) were directly induced by colchicine (Table 1). In water treatment (HV5CK vs HV0), novel_mir75, novel_mir56, novel_mir21

Table 1 The comparison of differentially expressed miRNAs and normal growth group in water treatment and colchicine treatment

Sample no.	miRNA ID	HV5CK vs HV0	HV5TR vs HV0
Differential expression in both groups of controls			
1	novel_mir21	↑	↑
2	nonel_mir56	↑	↑
3	novel_mir3	↓	↓
4	novel_mir38	↓	↑
Differential expression only in HV5CK vs HV0			
5	novel_mir69	↓	↓[a]
6	novel_mir57	↓	↓[a]
7	novel_mir75	↑	↓[a]
Differential expression only in HV5TR vs HV0			
8	novel_mir25	↓[a]	↓
Only detected and differentially expressed in HV5TR vs HV0			
9	novel_mir37	Not detected	↑

↑ Upregulated miRNAs, ↓ downregulated miRNAs

Not detected miRNAs that were not expressed

[a]miRNAs that were not significantly differentially expressed

Table 2 The differentially expressed miRNAs compared to water treatment

Sample no.	miRNA ID	HV5CK vs HV0	HV5TR vs HV5CK
Converse expression pattern			
1	novel_mir75	↑	↓
2	nonel_mir56	↑	↓
3	novel_mir69	↓	↑
4	novel_mir57	↓	↑
5	novel_mir38	↓	↑
Same expression pattern			
6	novel_mir3	↓	↓
7	novel_mir21	↑	↑
8	novel_mir25	↓[a]	↓
Only detected in HV5TR vs HV0			
9	novel_mir37	Not detected	↑

↑ Upregulated miRNAs, ↓ downregulated miRNAs

Not detected miRNAs which were not expressed

[a]miRNAs which were not significantly differentially expressed

were up-regulated, and novel_mir69, novel_mir57, novel_mir3, and novel_mir38 were down-regulated. When colchicine was included in solution (HV5TR vs HV5CK), novel_mir3, novel_mir21, and novel_mir25 had the same expression pattern in both water and colchicine treatments. However, novel_mir69, novel_mir57, novel_mir75, novel_mir38, and novel_mir56 showed the opposite expression patterns as those in water treatment (HV5CK vs HV0), In addition, novel_mir37 was up-regulated only in colchicine treatment (HV5TR vs HV0), but not in water treatment (Table 2).

Gene Ontology (GO) and KEGG function analysis of target genes

The function of the targets of nine differentially expressed miRNAs in HV5TR vs HV5CK was annotated, and these target genes were divided into three different categories based on their functions: biological processes, cellular components and molecular functions (Fig. 3a). Among all these possible target genes, the interesting findings were that novel_mir69, novel_mir56, and novel_mir25 commonly target the genes for DNA repair (Table 3), and are involved in DNA repair caused by mutation and injury as well as the process of nuclear transcriptional mRNA catabolism—nonsense-mediated decay, including inter-strand cross-linking repair, telomere capping, protection from non-homologous end joining of telomeres, telomere maintenance to cope with DNA damage. These GOs present the highest and extreme enrichment situation in all enriched GOs, which might be related to the toxicity caused by colchicine. Novel_mir38 targets actin, including positive regulation of cytoskeletal organization and protein polymerization as well as actin filament polymerization, Arp2/3 complex-mediated actin nucleation, actin nucleation, actin-based processes, actin cytoskeletal organization. Novel_mir21 targets the synthesis and development of high molecular substance in cell walls and cellular components; novel_mir75 targets protein kinase regulation and phosphorylation; novel_mir37 targets the genes involving the process of synthesis and metabolism of amino acid; novel_mir3 targets osmotic reactions as well as the repair of stress damage, which might also be related to the dimethyl sulfone that was added into solution. No predicted target was found for novel_mir57. KEGG pathway enrichment analysis revealed that these target genes are enriched in 20 pathways, including phenylpropanoid biosynthesis, plant-pathogen interaction, RNA transport, spliceosome, ABC transporters, pentose and glucuronate interconversions (Fig. 3b).

qRT-PCR analysis of differentially expressed miRNA

To validate high-throughput sequencing results and verify the expression pattern of novel miRNAs detected in sequencing, the sample '11z37' treated with 5 h of water (5hCK) and colchicine (5hTR) were used to validate 8 differentially expressed novel miRNAs in HV5TR vs HV5CK. Compared with '11z37' CK, the expressions of novell-mir69, novel_mir21 and novel_mir37 were up-regulated, and the expressions of novel_mir56, novel_mir75, novel_mir25 and novel_mir3 were down-regulated in 5hTR. The differentially

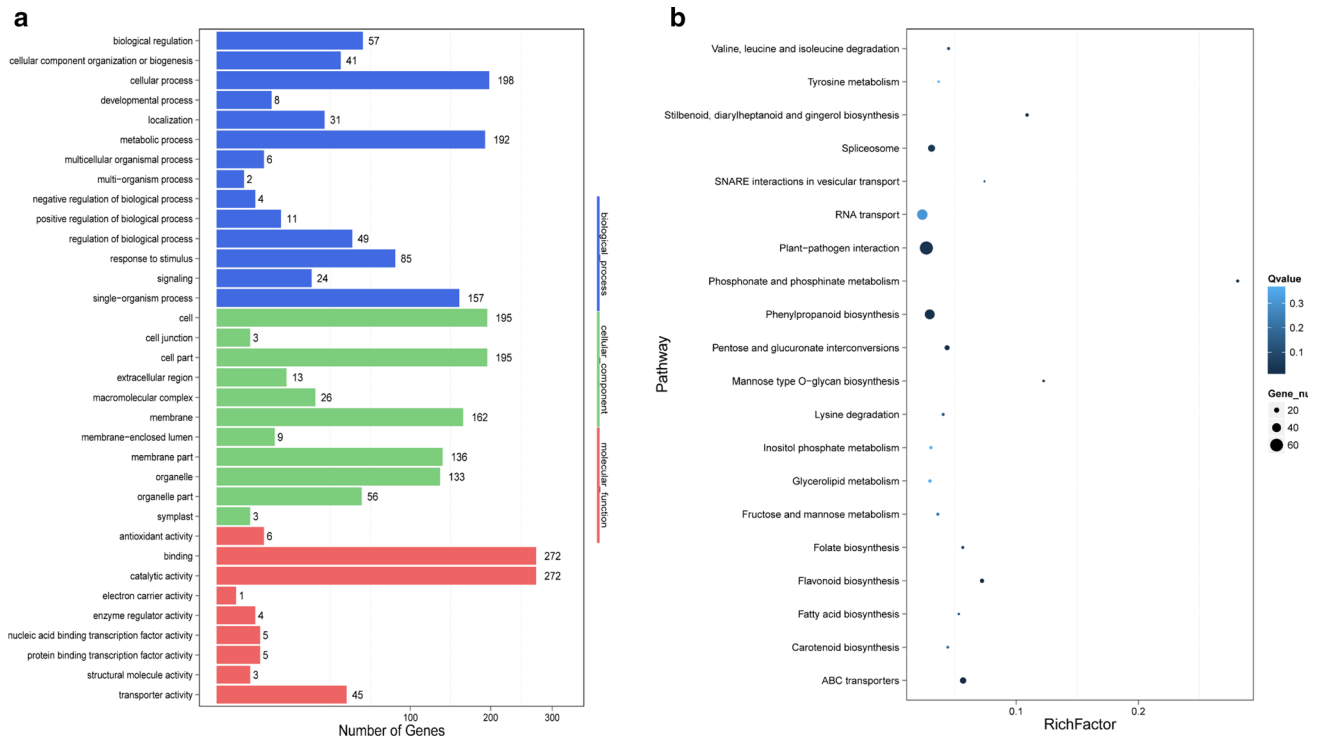

Fig. 3 GO and KEGG diagrams of target genes of differentially expressed miRNA compared in HV5TR vs HV5CK. **a** Gene ontology (GO) analysis of target genes of differentially expressed miRNAs in HV5TR vs HV5CK. **b** Kyoto Encyclopedia of Genes and Genomes (KEGG) analysis of target genes of differentially expressed miRNAs in HV5TR vs HV5CK

Table 3 Gene Ontology (GO) analysis of potential targets of three novel miRNAs associated with DNA repair

miRNA ID	Target gene	GO annotation	miRNA ID	Target gene	GO annotation
novel_mir56	MLOC_63780.14		novel_mir69	MLOC_13256.3	
	MLOC_63780.4			MLOC_4523.6	
	MLOC_73320.3			MLOC_13256.2	
	MLOC_63780.5			MLOC_13256.1	
	MLOC_63780.8			MLOC_13256.6	
	MLOC_63780.6			MLOC_13256.4	GO:0006281 DNA repair
	MLOC_73320.4			MLOC_13256.9	
	MLOC_63780.7			MLOC_13256.5	
	MLOC_63780.12	GO:0006281 DNA repair		MLOC_13256.7	
	MLOC_73320.5			MLOC_13256.8	
	MLOC_63780.3		novel_mir25	MLOC_54452.7	
	MLOC_73320.6			MLOC_54452.4	
	MLOC_63780.9			MLOC_54452.3	GO:0006281 DNA repair
	MLOC_63780.17			MLOC_54452.5	
	MLOC_73320.2			MLOC_54452.6	
	MLOC_73320.1				
	MLOC_63780.16				
	MLOC_63780.13				

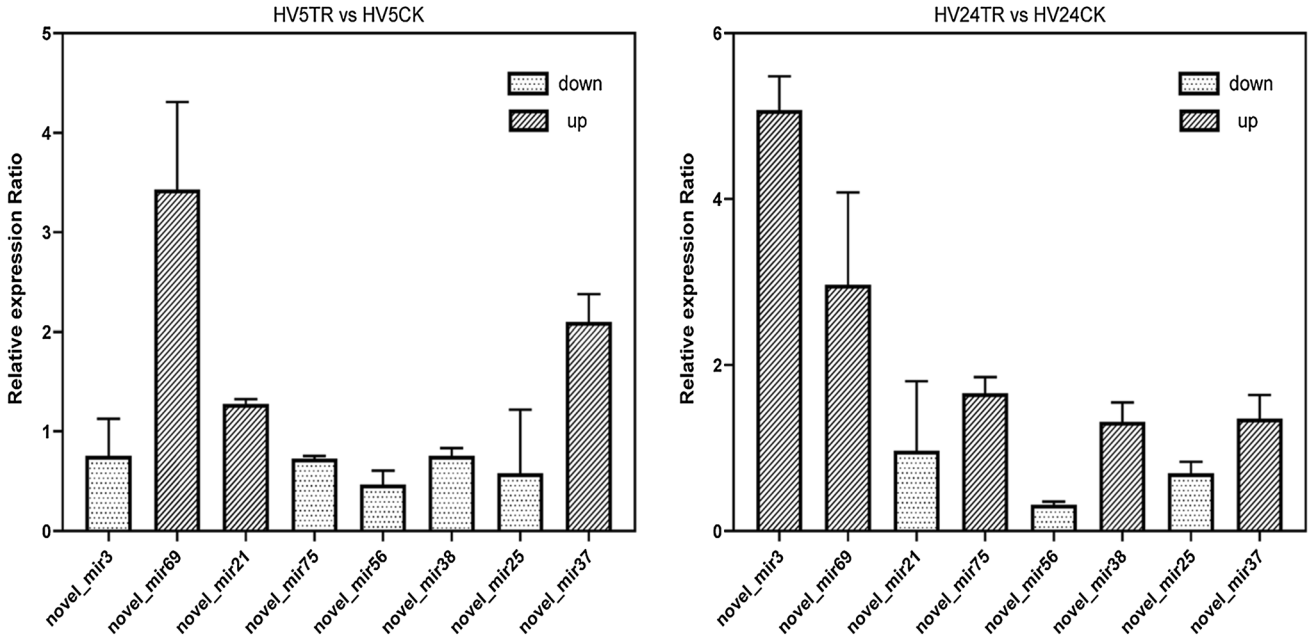

Fig. 4 qRT-PCR validation of differentially expressed miRNA detected by miRNA sequencing. Data represented are mean values ±SD ($n = 3$) from three biological replicates. **a** Bar graph illustrating the miRNAs with the same expression trend as the sequencing data in HV5TR vs HV5CK using qRT-PCR except novel_mir38. **b** The relative expression patterns of novel miRNA in the samples under 24 h colchicine solution treatment. The expression patterns of novel_mir3, novel_mir21, novel_mir75 and novel_mir38 were opposite to that in 5 h treatment (see **a**)

expression of these new miRNAs showed the same trend with the sequencing data (Fig. 4a). However, the expression level of novel_mir38 was slightly different from the sequencing data, which might be due to the sensitivity and specificity of the two techniques.

To reveal changes in miRNA expression under prolonged treatment, 8 differentially expressed novel miRNAs were tested in 24 h of water treatment and 24 h of colchicine (TR) treatment. The result showed that after 24 h treatment, the expression patterns of novel_mir3, novel_mir21, novel_mir75 and novel_mir38 were the opposite to the patterns in the 5 h treatment, and the expression of the remaining miRNAs was consistent with the results in the 5 h treatment (Fig. 4a, b).

qRT-PCR analysis of predicted targets of miRNA

In most cases, the identified miRNAs can cleave two or more different targets in target gene predictions. In our prediction, 8 differentially expressed novel miRNAs were predicted to target 1047 genes. To confirm whether miRNAs regulate their potential targets during colchicine treatment, we used qPCR to analyze the expressions patterns of 33 predicted target genes with DNA repair function that are co-targeted by novel_mir69, novel_mir56, and novel_mir25 in the GO enrichment analysis. As expected, we observed an inverse relationship between the two miRNAs (novel_mir69 and novel_mir56) and their predicted target genes (Fig. 5a, b), suggesting that they are potential miRNA-mediated targets. The expression of novel miRNA novel_mir25 and its predicted target genes did not show inverse relationship, suggesting that the predicted target genes for novel_mir25 might not be the real target.

Discussion

Colchicine treatment induces much small size of RNAs

By analyzing the length distribution of miRNAs in three libraries (HV0, HV5hCK, HV5hTR), we found rich small RNA distribution of 16 nt, 18-20 nt in HV5hTR (Fig. S1 c); The size of 18-20nt sRNA has been detected in previous sRNA-seq studies (Hsieh et al. 2009; Chen et al. 2011; Hackenberg et al. 2012; Alves et al. 2016; Cognat et al. 2017; Martinez et al. 2017). Among small RNA detected in roots and buds of *Arabidopsis* under normal and phosphorus deficiency, 19–20 nt tsRNAs (tRNA-derived small RNA) were detected, and the 19 nt 5′ tRF-Gly^{TCC} in the root accounted for 18–28% sRNA (Hsieh et al. 2009).

In our study, we found an enrichment of 16 nt sRNA. Two libraries from the HV5hTR showed abundant distribution of 16 nt, with a high degree of enrichment. In addition, one of

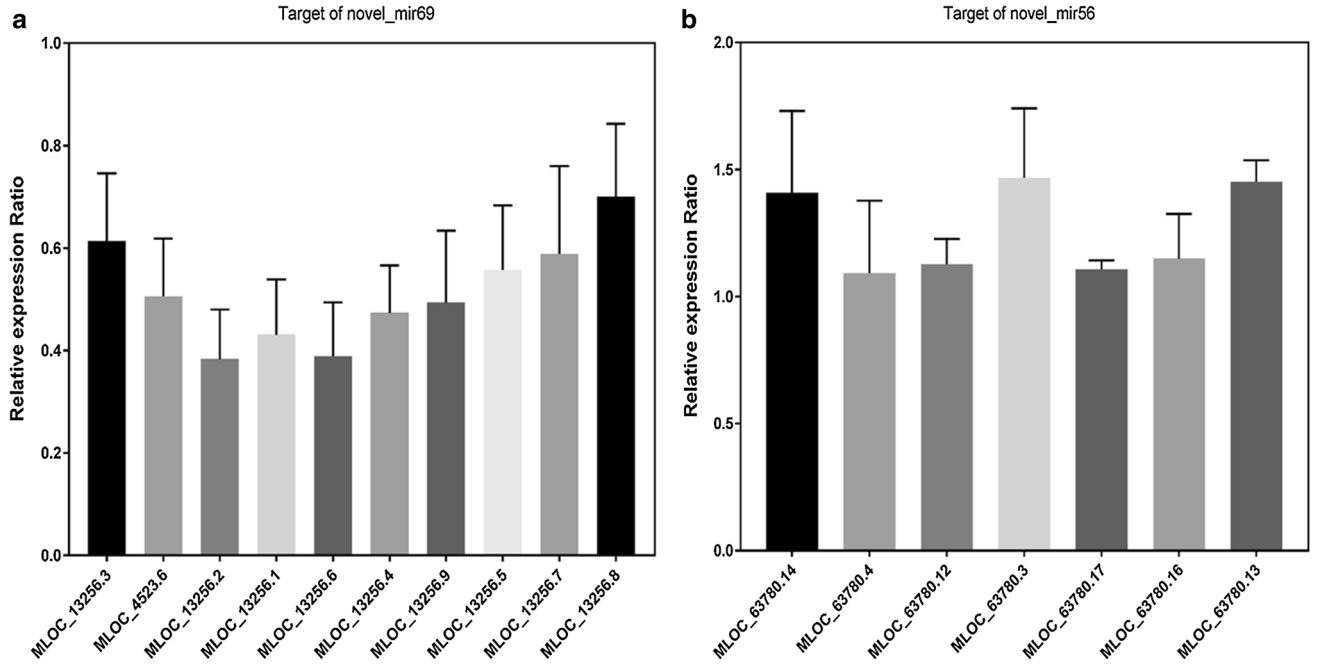

Fig. 5 qRT-PCR analysis of the genes targeted by two miRNAs. The graph shows the relative expression level of 5 h colchicine treatment/5 h CK. Data are mean values ± SD ($n = 3$) from three biological replicates. **a** The relative expression pattern of the novel_mir69 and its target genes showed inverse expression pattern. The novel_mir69 was up-regulated, its targeted genes were down-regulated. **b** The relative expression pattern of the novel_mir56 and its target genes showed inverse expression pattern. The novel_mir56 was down-regulated, its targeted genes were up-regulated

the three libraries from HV0 also had a 16 nt anomalous distribution. Baldrich et al. (2019) reported that single-stranded sRNA-"tyRNA" of 10–17 nt was abundant in extracellular vesicles from *Arabidopsis* rosette leaves, most of them were 16–17 nt. These tyRNAs were suggested to be derived from a variety of sources of degradation products, including mRNA, primary miRNAs, siRNAs, tasiRNAs and hcRNAs, and whether this RNA has cellular function or represents the waste and by-products of cellular metabolism remains unknown (Baldrich et al. 2019). In our study, a small number of 16 nt sRNAs were generated in one control group, which might be caused by slightly degradation of our RNA samples. However, 16 nt sRNAs were abundantly enriched in the colchicine treated samples, which cannot only be explained by the degradation of RNAs during handling RNA process. We speculated that colchicine might function on producing small strand of RNA, to confirm this, more studies are needed in future.

The same miRNA has different expression patterns in different treatments

In this study, most of the miRNAs in the water treatment and colchicine solution treatment showed a consistent expression pattern. Comparing the colchicine treatment group with the water treatment group, we found an interesting phenomenon as shown in Table 2, seven novel miRNAs were affected by water treatment, but more influenced by colchicine. Three and four novel miRNAs were up-regulated and down-regulated by water treatment, respectively. However, when colchicine was added to solution (HV5TR vs HV5CK), novel_mir69, novel_mir57, novel_mir75, novel_mir38, and novel_mir56 showed the opposite expression patterns as those in only treated with water (HV5CK vs HV0). The different expression patterns between HV5TR vs HV5CK and HV5CK vs HV0 might be caused by different stresses that plants suffered. In the HV5CK, the plants only suffered water stress, while in HV5TR, the plants suffered water, colchicine and combination of water and colchicine stresses. In a study on the response of tomato plants to a combination of heat and salt stress, Rivero et al. (2014) found that the expression of some transcripts under salt + heat treatment was only shared with the salinity treatment (as *LeOAT* and *LeNI*) or with the heat treatment (as *LePDH*, *LeBADH*, *LeCMO*), while under the stress combination treatment, *LeP5CS*, *LePO*, *LeSPS*, *LeFBPase* and *LeT6PS* showed an expression pattern that was specific and different from that found under salinity or heat treatments. It has been reported that in *Arabidopsis thaliana*, miR169 mediates the regulation of its target gene *NFYA5* that was significantly up-regulated under drought stress, and either silencing *NFYA5* gene or overexpressing miR169 in Arabidopsis reduced drought

tolerance and increase water loss (Li et al. 2008). On the contrary, when the expression of miR169 was decreased, the drought tolerance of *Arabidopsis thaliana* was enhanced, indicating that miR169 participates in the process of drought tolerance response of *Arabidopsis* mainly by mediating the regulation of the target gene *NFYA5* (Li et al. 2008). However, miR169 showed an opposite expression pattern in response to salt stress in *Arabidopsis*, which was up-regulated under salt stress conditions, while its target gene *NFYA5* was down-regulated (Xu et al. 2014). Other studies have shown that *Arabidopsis* miR398 was down-regulated under ABA induction and salt stress, but up-regulated under drought treatment, and its target gene copper superoxide dismutase (CSD) was up-regulated under salt stress (Sunkar et al. 2006; Jia et al. 2009).

Potential targets for differentially expressed miRNAs

Early studies on *Arabidopsis* indicated that the potential targets for most miRNAs were transcription factors (Chen et al. 2012), and participated in complex gene regulatory networks (Navarro et al. 2006). GO and KEGG enrichment analyses were performed on the predicted genes targeted by these 8 differentially expressed novel miRNAs. In the KEGG enrichment analysis, we found that the pathway of phenylpropanoid synthesis in the enrichment pathway coincides with the transcriptome data derived from colchicine treated diploid orchardgrass (Zhou et al. 2017). It was suggested that the high mortality rate of plants treated with colchicine is due to the large scale of down-regulation of phenylpropanoid synthesis genes (Zhou et al. 2017). The consensus results of transcriptome and miRNA indicated that miRNA plays an important role in pathway of phenylpropanoid synthesis (Table S5).

Previous studies indicated that colchicine inhibits the formation of microtubules, leading to the abnormal division of cells (Leblanc et al. 1995; Liu et al. 2007). Yet we do not have a clear answer on how cells respond to colchicine treatment at the molecular level. In our GO enrichment analysis, most of the targets of novel_mir38 are actin, and novel_mir21 targets the synthesis of macromolecules such as cell walls. It is now generally accepted that colchicine inhibits the formation of spindle mainly by inhibiting microtubules, and then inhibits mitosis (Nebel 1937). However, it has been reported that dynamic assembly of F-actin is involved in the occurrence of abnormal mitosis in cells after UV-B irradiation (Chen and Han 2015). Studies have shown that during the process of cell division, actin filaments form a cytoplasmic chain that crosses the vacuole to connect the cytoplasm and cortical cytoplasm around the nucleus to ensure normal division (Smith 2001). In the process of late cytokinesis, microfilaments can also ensure precise division by maintaining the spatial localization of daughter nuclei (Lénárt et al. 2005). In the mitosis of higher plants, the prephase band (PBB) is formed by cortical microtubules and microfilaments thus determining the dividing surface of the cells (Smith 2001). It has been reported when the GFP-mTalin (mouse talin) fusion protein was transferred into tobacco cells, at the late stage of mitosis, the formation of tobacco cell plates depends on microfilaments (Yu et al. 2006), and the position of the cell plate also has a film-forming body formed by microfilament and microtubules. During cytokinesis, the film-forming body composed of microtubules and microfilaments in plants directs vesicles to transport material from the cell wall to form new cell walls (Jürgens 2005; Dhonukshe et al. 2006), and the subsequent synthesis and transport of hemicellulose and lignin gradually form the mature cell wall that can divide cell.

As a toxic mitotic inhibitor, colchicine can cause a high mortality rate to plants, and plants undergo a large number of programmed deaths in response to this kind of severe external stress. A number of reports indicated that plant cell cytoskeleton responds to programmed cell death (PCD) by reassembly, primarily by re-establishing the morphological distribution of microtubules and microfilaments. In most cases, the microtubule skeleton depolymerizes, and the microfilament skeleton can be rebuilt in two ways, either form a stable aggregation point after agglomeration, or depolymerize after forming a microfilament bundle (Smertenko and Franklin-Tong 2011). The novel_mir75 targets the genes regulating protein kinase and phosphorylation which control cyclin. It is now known that cyclin kinase (CDK) is a central regulatory organ in the plant cell cycle, and CDK activity becomes very high during the G1/S and G2/M boundary periods, which is associated with massive protein phosphorylation (Lew and Kornbluth 1996). Therefore, we propose a network that novel_38, novel_21 and novel_mir75 jointly respond to the abnormal process of cell division under colchicine treatment (Fig. 6a).

Novel_mir3 targets the repair of stress damage; colchicine solution is usually used directly to treat exposed parts of plants, so it brings serious water osmotic pressure and alkaloid toxicity to plants. Plants grow in hypoxic environment, and anaerobic respiration of roots accumulate ethanol. It has been reported that the expression of alcohol dehydrogenase (ADH) gene was increased in a hypoxic environment (Wignarajah et al. 1976). The transcriptome provided by Zhou et al. (2017) demonstrated that ADH in colchicine treatment was significantly down-regulated compared with water treatment, suggesting that colchicine can reduce the pressure of waterlogging. Our results suggested that novel_mir3 might be involved in response to hypoxia. The novel_mir37 targets the synthesis and metabolism of amino acids, and plant amino acid metabolism can cope with the effects of abiotic stress. It has been reported that methionine metabolism

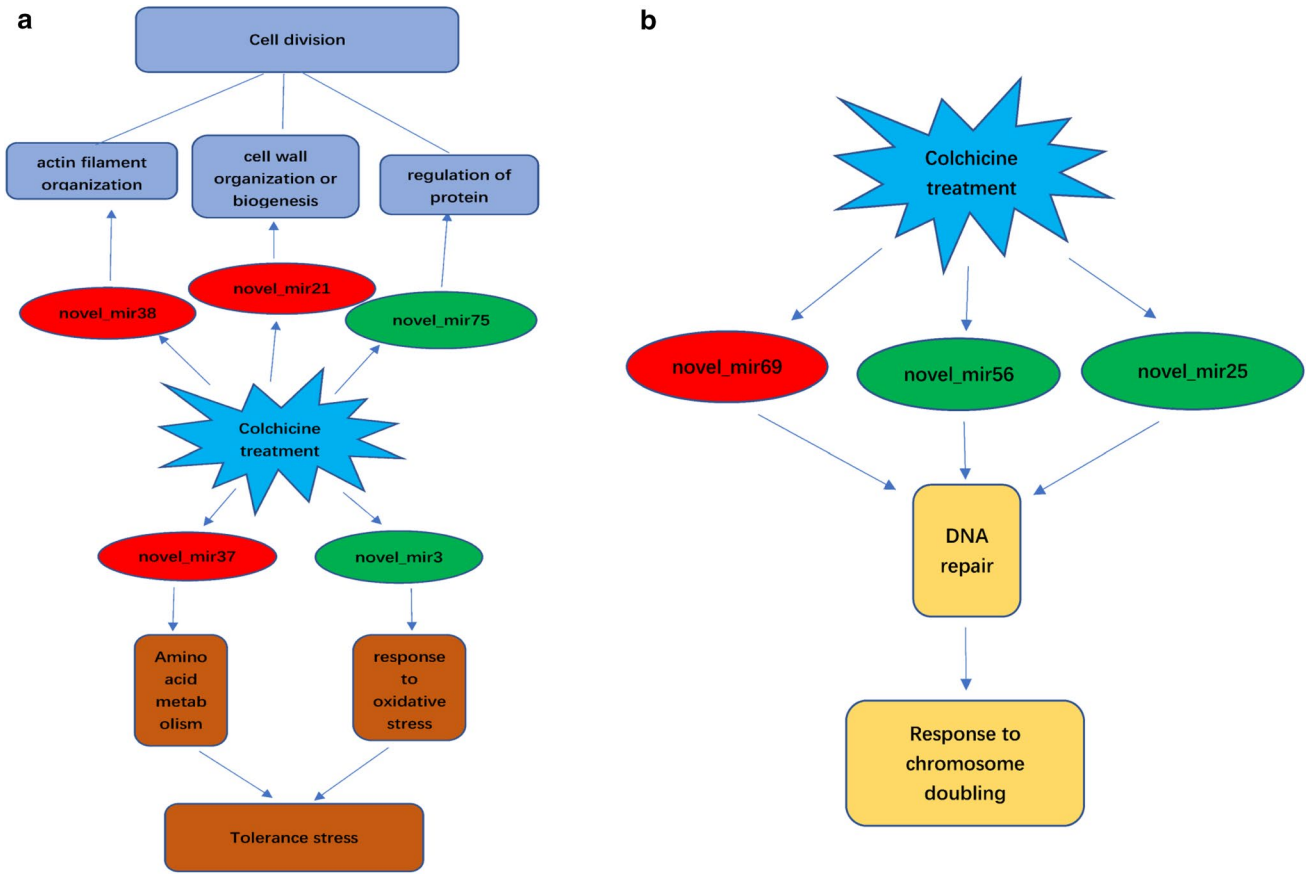

Fig. 6 Hypothetical network of miRNAs-mediated responses to colchicine treatment in plants. Red represents up-regulation; green represents down-regulation. **a** Hypothetical network that novel_38, novel_21 and novel_mir75 jointly respond to the abnormal process of cell division under colchicine treatment. **b** Response to chromosome doubling. The novel miRNAs involved in the DNA repair pathway in the treatment of colchicine

responds to the salt stress in *Arabidopsis* (Less and Galili 2008). The transcriptome analysis of colchicine treated plant showed that the amino acid metabolism in the colchicine treatment group was also significantly increased (Zhou et al. 2017). The specific mechanism and correlation between the amino acid metabolism and novel_mir37 in response to colchicine treatment remain to be explored in future.

In summary, our results suggested that novel_mir38, novel_21, novel_mir75, novel_mir37, and novel_mir3 might together regulate the abnormal process of cell division under colchicine treatment (Fig. 6a).

Potential targets associated with DNA damage repair

This study identified 9 novel miRNAs that were differentially expressed under colchicine treatment. GO analysis indicated that their many potential target genes play an important role in a variety of biological regulation processes, especially in DNA damage repair. qRT-PCR analysis showed that under the treatment of colchicine, the expressions of 2 novel miRNAs in the barley roots were inversely related to expression of the predicted 17 target genes. Artificially synthesized polyploids using colchicine could cause DNA mutation, but recent studies have rejected this hypothesis and proven that polyploid genomic structural variation has nothing to do with colchicine (Parisod et al. 2010). A recent DNA-SRAP analysis of the tetraploid *Chrysanthemum* induced by colchicine showed that 1.6% of new fragments and 1.1% of missing fragments appeared in newly synthesized tetraploid (Gao et al. 2016). A new synthetic autopolyploid phlox study showed that the first generation of autopolyploid produced 17% DNA deletion, and by the third generation it had 25% DNA deletions (Raina et al. 1994). A study on *Elymus elongatus* showed that 10% DNA deletion occurred in both artificial and natural formatting autopolyploid (Eilam et al. 2009). Research on *Paspalum notatum* also revealed that its DNA has a 9.5% deletion (Martelotto et al. 2007). Genomic structural variations between the existing autopolyploid and its ancestral diploid was detected in *Arabidopsis* (Santos et al. 2003). In our study, we found that 3 novel miRNAs were involved in the DNA repair pathway

in the treatment of colchicine (Fig. 6b), but the exact function of the target genes is still unknown. Therefore, we speculated that their target genes might involve in the process of plant cell DNA deletion and genomic structural variation under colchicine treatment. The results presented here will be useful for further functional analysis of these novel miRNAs and their target genes.

Author contribution statement GS and DW conceived and designed research. FS, LL, YY, XR and QH conducted experiments. GS, DW and CYW contributed new reagents or analytical tools. FS and GS analyzed data and wrote the manuscript. All authors read and approved the manuscript.

Acknowledgements This study was financially supported by the National Key Research and Development Program of China (2017YFD0301304) and the international Science and Technology Cooperation Projects of Anhui Province (1704e1002232) to DW, a Research Foundation for Talented Scholars from Anhui Agricultural University and the introduced leading talent research team for Universities in Anhui Province, the Natural Sciences and Engineering Research Council of Canada (RGPIN-2018-05433) to GS.

Compliance with ethical standards

Conflict of interest The authors declare that they have no competing financial interests.

References

Alves CS, Vicentini R, Duarte GT, Pinoti VF, Vincentz M, Nogueira FTS (2016) Genome-wide identification and characterization of tRNA-derived RNA fragments in land plants. Plant Mol Biol 93(1–2):1–14

Baldrich P, Rutter BD, Karimi HZ, Podicheti R, Meyers BC, Innes RW (2019) Plant extracellular vesicles contain diverse small RNA species and are enriched in 10-to 17-nucleotide "tiny" RNAs. Plant Cell 31(2):315–324

Bardou P, Mariette J, Escudié F, Djemiel C, Klopp C (2014) jvenn: an interactive Venn diagram viewer. BMC Bioinform 15(1):293

Barnabás B, Obert B, Kovács G (1999) Colchicine, an efficient genome-doubling agent for maize (*Zea mays* L.) microspores cultured in anther. Plant Cell Rep 18(10):858–862

Bian H, Xie Y, Guo F, Han N, Ma S, Zeng Z, Wang J, Yang Y, Zhu M (2012) Distinctive expression patterns and roles of the miRNA393/TIR1 homolog module in regulating flag leaf inclination and primary and crown root growth in rice (*Oryza sativa*). New Phytol 196(1):149–161

Blakeslee AF, Avery AG (1937) Methods of inducing doubling of chromosomes in plants: by treatment with colchicine. J Hered 28(12):393–411

Chen H, Han R (2015) F-actin participates in the process of the "partition-bundle division". Russ J Plant Physiol 62(2):187–194

Chen C-J, Qing L, Yu-Chan Z, Liang-Hu Q, Yue-Qin C, Daniel G (2011) Genome-wide discovery and analysis of microRNAs and other small RNAs from rice embryogenic callus. RNA Biol 8(3):538–547

Chen L, Wang T, Zhao M, Tian Q, Zhang WH (2012) Identification of aluminum-responsive microRNAs in *Medicago truncatula* by genome-wide high-throughput sequencing. Planta 235(2):375–386

Cognat V, Morelle G, Megel C, Lalande S, Molinier J, Vincent T, Small I, Duchêne AM, Maréchaldrouard L (2017) The nuclear and organellar tRNA-derived RNA fragment population in *Arabidopsis thaliana* is highly dynamic. Nucleic Acids Res 45(6):3460–3472

Dhonukshe P, Baluška F, Schlicht M, Hlavacka A, Šamaj J, Friml J, Gadella TW Jr (2006) Endocytosis of cell surface material mediates cell plate formation during plant cytokinesis. Dev Cell 10(1):137–150

Dhooghe E, Van Laere K, Eeckhaut T, Leus L, Van Huylenbroeck J (2011) Mitotic chromosome doubling of plant tissues in vitro. Plant Cell Tissue Organ Cult 104(3):359–373

Eilam T, Anikster Y, Millet E, Manisterski J, Feldman M (2009) Genome size in natural and synthetic autopolyploids and in a natural segmental allopolyploid of several Triticeae species. Genome 52(3):275–285

Evers M, Huttner M, Dueck A, Meister G, Engelmann JC (2015) miRA: adaptable novel miRNA identification in plants using small RNA sequencing data. BMC Bioinform 16(1):370

Finkelstein Y, Aks SE, Hutson JR, Juurlink DN, Nguyen P, Dubnov-Raz G, Pollak U, Koren G, Bentur Y (2010) Colchicine poisoning: the dark side of an ancient drug. Clin Toxicol 48(5):407–414

Gao R, Wang H, Dong B, Yang X, Chen S, Jiang J, Zhang Z, Liu C, Zhao N, Chen F (2016) Morphological, genome and gene expression changes in newly induced autopolyploid *Chrysanthemum lavandulifolium* (Fisch. ex Trautv.) Makino. Int J Mol Sci 17(10):1690

Hackenberg M, Huang PJ, Huang CY, Shi BJ, Gustafson P, Langridge P (2012) A comprehensive expression profile of microRNAs and other classes of non-coding small RNAs in barley under phosphorous-deficient and -sufficient conditions. DNA Res 20(2):109–125

Hastie SB (1991) Interactions of colchicine with tubulin. Pharmacol Therapeut 51(3):377–401

Heinz DJ, Mee GW (1970) Colchicine-induced polyploids from cell suspension cultures of sugarcane. Crop Sci 10(6):696–699

Hsieh LC, Lin SI, Shih ACC, Chen JW, Lin WY, Tseng CY, Li WH, Chiou TJ (2009) Uncovering small RNA-mediated responses to phosphate deficiency in Arabidopsis by deep sequencing. Plant Physiol 151(5):2120–2132

Iwakawa H-O, Tomari Y (2013) Molecular insights into microRNA-mediated translational repression in plants. Mol Cell 52(4):591–601

Jia X, Wang WX, Ren L, Chen QJ, Mendu V, Willcut B, Dinkins R, Tang X, Tang G (2009) Differential and dynamic regulation of miR398 in response to ABA and salt stress in *Populus tremula* and *Arabidopsis thaliana*. Plant Mol Biol 71(1–2):51–59

Jürgens G (2005) Cytokinesis in higher plants. Annu Rev Plant Biol 56:281–299

Katiyar A, Smita S, Muthusamy SK, Chinnusamy V, Pandey DM, Bansal KC (2015) Identification of novel drought-responsive microRNAs and trans-acting siRNAs from *Sorghum bicolor* (L.) Moench by high-throughput sequencing analysis. Front Plant Sci 6:506

Knauer S, Holt AL, Rubio-Somoza I, Tucker EJ, Hinze A, Pisch M, Javelle M, Timmermans MC, Tucker MR, Laux T (2013) A protodermal miR394 signal defines a region of stem cell competence in the *Arabidopsis* shoot meristem. Develop Cell 24(2):125–132

Leblanc O, Duenas M, Hernandez M, Bello S, Garcia V, Berthaud J, Savidan Y (1995) Chromosome doubling in *Tripsacum*: the production of artificial, sexual tetraploid plants. Plant Breed 114(3):226–230

Lénárt P, Bacher CP, Daigle N, Hand AR, Eils R, Terasaki M, Ellenberg J (2005) A contractile nuclear actin network drives chromosome congression in oocytes. Nature 436(7052):812

Less H, Galili G (2008) Principal transcriptional programs regulating plant amino acid metabolism in response to abiotic stresses. Plant Physiol 147(1):316–330
Lew DJ, Kornbluth S (1996) Regulatory roles of cyclin dependent kinase phosphorylation in cell cycle control. Curr Opin Cell Biol 8(6):795–804
Li W, Hu D-n, Li H, Chen X-Y (2007) Polyploid induction of *Lespedeza formosa* by colchicine treatment. Forest Stud China 9(4):283–286
Li WX, Oono Y, Zhu JH, He XJ, Wu JM, Iida K, Lu XY, Cui XP, Jin HL, Zhu JK (2008) The *Arabidopsis* NFYA5 transcription factor is regulated transcriptionally and posttranscriptionally to promote drought resistance. Plant Cell 20(8):2238–2251
Liu B, Sun G (2017) microRNAs contribute to enhanced salt adaptation of the autopolyploid *Hordeum bulbosum* compared with its diploid ancestor. Plant J 91(1):57–69
Liu G, Li Z, Bao M (2007) Colchicine-induced chromosome doubling in *Platanus acerifolia* and its effect on plant morphology. Euphytica 157(1–2):145–154
Liu Q, Yao X, Pi L, Wang H, Cui X, Huang H (2009) The *Argonaute10* gene modulates shoot apical meristem maintenance and establishment of leaf polarity by repressing miR165/166 in Arabidopsis. Plant J 58(1):27–40
Martelotto LG, Ortiz JPA, Stein J, Espinoza F, Quarin CL, Pessino SC (2007) Genome rearrangements derived from autopolyploidization in *Paspalum* sp. Plant Sci 172(5):970–977
Martinez G, Choudury SG, Slotkin RK (2017) tRNA-derived small RNAs target transposable element transcripts. Nucleic Acids Res 45(9):5142–5152
Nakajima Y, Suzuki S (2013) Environmental stresses induce misfolded protein aggregation in plant cells in a microtubule-dependent manner. Intl J Mol Sci 14(4):7771–7783
Navarro L, Dunoyer P, Jay F, Arnold B, Dharmasiri N, Estelle M, Voinnet O, Jones JDG (2006) A plant miRNA contributes to antibacterial resistance by repressing auxin signaling. Science 312(5772):436
Nebel BR (1937) Mechanism of polyploidy through colchicine. Nature 140(3556):1101
Nogales E, Wolf S, Downing K (1998) Structure of the *ab* tubulin dimer by electron crystallography (Correction). Nature 393(6681):191
Pan W, Houben A, Schlegel R (1993) Highly effective cell synchronization in plant roots by hydroxyurea and amiprophos-methyl or colchicine. Genome 36(2):387–390
Parisod C, Holderegger R, Brochmann C (2010) Evolutionary consequences of autopolyploidy. New Phytol 186(1):5–17
Petersen KK, Hagberg P, Kristiansen K, Forkmann G (2002) In vitro chromosome doubling of *Miscanthus sinensis*. Plant Breed 121(5):445–450
Pfaffl MW (2001) A new mathematical model for relative quantification in real-time RT–PCR. Nucleic Acids Res 29(9):e45–e45
Raina SN, Parida A, Koul KK, Salimath SS, Bisht MS, Raja V, Khoshoo TN (1994) Associated chromosomal DNA changes in polyploids. Genome 37(4):560–564
Rivero RM, Mestre TC, Mittler R, Rubio F, Garcia-Sanchez F, Martinez V (2014) The combined effect of salinity and heat reveals a specific physiological, biochemical and molecular response in tomato plants. Plant Cell Environ 37(5):1059–1073
RStudio Team (2015) RStudio: Integrated development for R. RStudio, Inc., Boston, MA (Computer software v0.98.1074), http://www.rstudio.com/. Accessed 30 Jan 2019
Santos J, Alfaro D, Sanchez-Moran E, Armstrong S, Franklin F, Jones G (2003) Partial diploidization of meiosis in autotetraploid *Arabidopsis thaliana*. Genetics 165(3):1533–1540
Shi R, Chiang VL (2005) Facile means for quantifying microRNA expression by real-time PCR. Biotech 39(4):519–525
Smertenko A, Franklin-Tong VE (2011) Organisation and regulation of the cytoskeleton in plant programmed cell death. Cell Death Differ 18(8):1263–1270. https://doi.org/10.1038/cdd.2011.39
Smith LG (2001) Plant cell division: building walls in the right places. Nat Rev Mol Cell Biol 2(1):33
Sourour AR, Ameni B, Mejda C (2014) Efficient production of tetraploid barley (*Hordeum vulgare* L.) by colchicine treatment of diploid barley. J Exp Biol Agric Sci 2:113–119
Stief A, Altmann S, Hoffmann K, Pant BD, Scheible W-R, Bäurle I (2014) *Arabidopsis miR156* regulates tolerance to recurring environmental stress through *SPL* transcription factors. Plant Cell 26(4):1792–1807
Sunkar R, Zhu J-K (2004) Novel and stress-regulated microRNAs and other small RNAs from *Arabidopsis*. Plant Cell 16(8):2001–2019
Sunkar R, Girke T, Zhu J-K (2005) Identification and characterization of endogenous small interfering RNAs from rice. Nucleic Acids Res 33(14):4443–4454
Sunkar R, Kapoor A, Zhu J-K (2006) Posttranscriptional induction of two Cu/Zn superoxide dismutase genes in *Arabidopsis* is mediated by downregulation of miR398 and important for oxidative stress tolerance. Plant Cell 18(9):2415
Untergasser A, Cutcutache I, Koressaar T, Ye J, Faircloth BC, Remm M, Rozen SG (2012) Primer3—new capabilities and interfaces. Nucleic Acids Res 40(15):e115–e115
Wang J-J, Guo H-S (2015) Cleavage of *INDOLE-3-ACETIC ACID INDUCIBLE28* mRNA by microRNA847 upregulates auxin signaling to modulate cell proliferation and lateral organ growth in Arabidopsis. Plant Cell 27(3):574–590
Wei T, Wang Y, Xie Z, Guo D, Chen C, Fan Q, Deng X, Liu JH (2018) Enhanced ROS scavenging and sugar accumulation contribute to drought tolerance of naturally occurring autotetraploids in *Poncirus trifoliata*. Plant Biotech J. https://doi.org/10.1111/pbi.13064
Wignarajah K, Greenway H, John AD (1976) Effect of waterlogging on growth and activity of alcohol dehydrogenase in barley and rice. New Phytol 77(3):585–592
Winter J, Diederichs S (2011) Argonaute proteins regulate microRNA stability: increased microRNA abundance by Argonaute proteins is due to microRNA stabilization. RNA Biol 8(6):1149–1157
Xu Q, He Q, Li S, Tian Z (2014) Molecular characterization of *StNAC2* in potato and its overexpression confers drought and salt tolerance. Acta Physiol Plant 36(7):1841–1851
Yang C, Li D, Mao D, Liu X, Ji C, Li X, Zhao X, Cheng Z, Chen C, Zhu L (2013) Overexpression of microRNA319 impacts leaf morphogenesis and leads to enhanced cold tolerance in rice (*Oryza sativa* L.). Plant Cell Environ 36(12):2207–2218
Yu M, Yuan M, Ren H (2006) Visualization of actin cytoskeletal dynamics during the cell cycle in tobacco (*Nicotiana tabacum* L. cv Bright Yellow) cells. Biol Cell 98(5):295–306
Zhang B, Wang Q (2015) MicroRNA-based biotechnology for plant improvement. J Cell Physiol 230(1):1–15
Zhang J, Zhang M, Deng X (2007) Obtaining autotetraploids in vitro at a high frequency in *Citrus sinensis*. Plant Cell Tissue Organ Cult 89(2–3):211
Zhang X, Zou Z, Gong P, Zhang J, Ziaf K, Li H, Xiao F, Ye Z (2011) Over-expression of microRNA169 confers enhanced drought tolerance to tomato. Biotech Lett 33(2):403–409
Zhao M, Ding H, Zhu JK, Zhang F, Li WX (2011) Involvement of miR169 in the nitrogen-starvation responses in Arabidopsis. New Phytol 190(4):906–915
Zhou K, Fleet P, Nevo E, Zhang X, Sun G (2017) Transcriptome analysis reveals plant response to colchicine treatment during on chromosome doubling. Sci Rep 7(1):8503
Zhou K, Liu B, Wang Y, Zhang X, Sun G (2019) Evolutionary mechanism of genome duplication enhancing natural autotetraploid sea barley adaptability to drought stress. Environ Exp Bot 159:44–54